



Universiteit
Leiden
The Netherlands

Copper complexes as biomimetic models of catechol oxidase: mechanistic studies

Koval, I.A.

Citation

Koval, I. A. (2006, February 2). *Copper complexes as biomimetic models of catechol oxidase: mechanistic studies*. Retrieved from <https://hdl.handle.net/1887/4295>

Version: Corrected Publisher's Version

License: [Licence agreement concerning inclusion of doctoral thesis in the Institutional Repository of the University of Leiden](#)

Downloaded from: <https://hdl.handle.net/1887/4295>

Note: To cite this publication please use the final published version (if applicable).

3

Structural diversity in Cu^{II}, Co^{II} and Mn^{II} complexes of a phenol-based ligand containing amine, pyridine and formyl functions: 3D structures and solution studies.[†]

The phenol-based ligand Hpy2ald, prepared as an intermediate in the synthesis of the ligand Hpy3asym, described in Chapter 2, contains formyl, amine and pyridine functions. Its reaction with Cu^{II}, Mn^{II} and Co^{II} salts leads to complexes with very different structural features and different nuclearities. Depending on the counter ion, the carbonyl group of the ligand can be either bound to a metal ion, or remain non-coordinated, fully changing the ligand coordination behavior. In this chapter the 3D structures, solution and magnetic properties of six different complexes: [Co₂(py2ald)₂](ClO₄)₂·0.7CH₃OH (1), [Co₂(py2ald)₂](BF₄)₂·CH₃OH (2), [Mn₂(py2ald)₂](ClO₄)₂·C₄H₁₀O (3), [Cu(Hpy2ald)Br₂]·0.5H₂O (4), [Mn(Hpy2ald)Cl₂] (5) and [Cu₂(py2ald)(μ-NO₃)(NO₃)₂]·CH₃CN (6) are reported. In the first three complexes, two metal ions are doubly bridged by two deprotonated phenolate groups of two ligands, resulting in dinuclear structures, with the oxygen atom of the carbonyl group occupying one position in the metal coordination sphere. In the latter three complexes, the coordinating counter ions Br⁻, Cl⁻ and NO₃⁻ prevent a binding of the weaker donor (carbonyl group) to the metal centers, leading to complexes with a metal to ligand ratio of 2:2, 1:1, and 2:1, respectively. In the first two complexes, the phenol group of the ligand remains protonated and fails to bridge two metal ions, instead being semi-coordinated to only one metal ion.

[†]This chapter is based on: Koval, I. A.; Huisman, M.; Stassen, A. F.; Gamez, P.; Lutz, M.; Spek, A. L. Pursche, D.; Krebs, B. and Reedijk, J., *Inorg. Chim. Acta*, 2004, 357, 294-300, and Koval, I. A.; Huisman, M.; Stassen, A. F.; Gamez, P.; Lutz, M.; Spek, A. L.; and Reedijk, J. *Eur. J. Inorg. Chem.*, 2004, 591-600

3.1 Introduction

Some time ago, Adams *et al.* reported^{1,2} an unexpected nickel-induced hydrolysis of unsymmetrical Schiff base compartmental ligands, which resulted in the transformation of the imino group of the ligands into a formyl moiety. As this hydrolysis only occurred when nickel(II) salts with non- or weakly coordinating anions were used, it was suggested that the presence of such anions, as well as of nickel ions is crucial.² All dinuclear complexes, which were obtained with these *in situ* generated ligands, were found to have very similar crystal structures, comprised of a dimetal core with two bridging phenolato groups from two ligands. In all cases the metal to ligand ratio was found to be 2:2. The coordination environment around each metal ion was completed to a distorted octahedron by three nitrogen donor atoms from an amino arm of the ligand and an oxygen atom of the formyl group formed due to the hydrolysis.

In this chapter, six novel complexes of the phenol-based compartmental ligand Hpy2ald (Figure 3.1), containing formyl, amino and pyridine functions, with copper(II), cobalt(II) and manganese(II) ions are reported. The ligand Hpy2ald was prepared as an intermediate in the synthesis of the asymmetric dinucleating ligand Hpy3asym (Chapter 2).³ Three of the reported complexes ($[\text{Co}_2(\text{py2ald})_2](\text{ClO}_4)_2 \cdot 0.7\text{CH}_3\text{OH}$ (**1**), $[\text{Co}_2(\text{py2ald})_2](\text{BF}_4)_2 \cdot \text{CH}_3\text{OH}$ (**2**) and $[\text{Mn}_2(\text{py2ald})_2](\text{ClO}_4)_2 \cdot \text{C}_4\text{H}_{10}\text{O}$ (**3**)) possess a structure very similar to those reported by Adams *et al.*,^{1,2} whereas the other three complexes, namely $[\text{Cu}(\text{Hpy2ald})\text{Br}_2] \cdot 0.5\text{H}_2\text{O}$ (**4**), $[\text{Mn}(\text{Hpy2ald})\text{Cl}_2]$ (**5**) and $[\text{Cu}_2(\text{py2ald})(\mu\text{-NO}_3)(\text{NO}_3)_2] \cdot \text{CH}_3\text{CN}$ (**6**), exhibit completely different structural features. The crystal structures, spectroscopic and magnetic properties of all six complexes are reported.

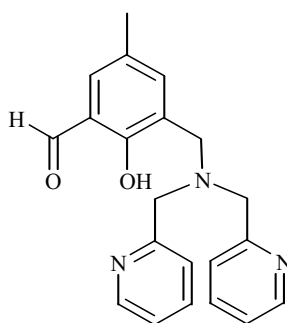


Figure 3.1. The phenol-based ligand Hpy2ald.

3.2 Results and Discussion

3.2.1 Crystal structure descriptions

$[\text{Co}_2(\text{py2ald})_2](\text{ClO}_4)_2 \cdot 0.7\text{CH}_3\text{OH}$ (**1**)

Pink rectangular blocks of the compound were obtained by diethyl ether diffusion into the methanol solution of the reactants. An ORTEP projection of the

complex cation $[\text{Co}_2(\text{py2ald})_2]^{2+}$ is shown in Figure 3.2. Selected bond lengths and angles are presented in Table 3.1. The compound crystallizes in the space group $Fdd2$, with sixteen formula units present per unit cell. The complex cation is constituted by two deprotonated ligands and two Co^{II} ions, resulting in a dimeric structure with a $\text{Co}\cdots\text{Co}$ separation of 3.2031(6) Å. Two cobalt ions are bridged by two μ -phenoxy bridges from two deprotonated cresolates, resulting in an almost ideal parallelogram formed by two *trans*-located cobalt ions Co1 and Co2 and two *trans*-located oxygen atoms O31 and O71. The distances Co1-O71 and Co2-O31 are approximately equal (2.0323(19) Å and 2.0344(19) Å, respectively), as well as the distances Co1-O31 and Co2-O71 (2.100(2) Å and 2.101(2) Å, respectively). The interior angles of the parallelogram are 78.32(7) and 78.25(8)° for O-Co-O and 101.57(8) and 101.55(9)° for Co-O-Co, and their sum amounts to 359.7°, which is very close to the planar value of 360°.

Both cobalt ions have a significantly distorted octahedral surrounding, accomplished by a N_3O_3 donor set. The coordination sphere of each ion is completed by two nitrogen atoms from two pyridine rings, a nitrogen donor from a tertiary amine group and an oxygen from the carbonyl group. For both ions, the oxygen atom from the deprotonated cresolate and the nitrogen atom from the tertiary amine group are occupying the axial positions, whereas two pyridine rings lie in the equatorial plane on either side of the ligand plane and thus are *trans*-located to each other.

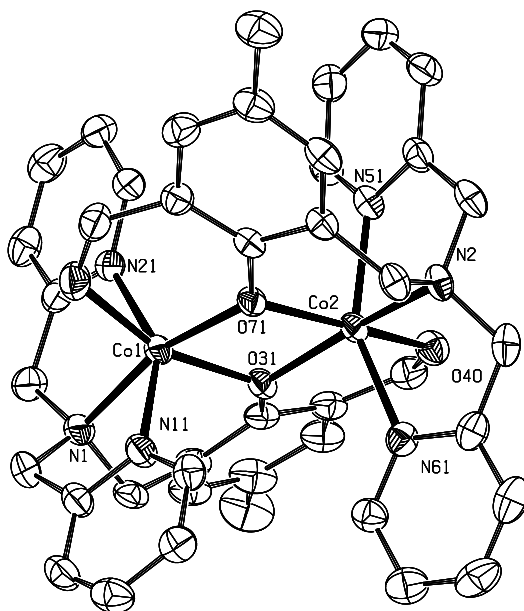


Figure 3.2. ORTEP projection of the dinuclear cation $[\text{Co}_2(\text{py2ald})_2]^{2+}$. Hydrogen atoms are omitted for clarity.

The doubly positive charge of the complex cation is compensated by perchlorate anions. One perchlorate is on a general position and two independent perchlorates are located on twofold axes. Additionally, 0.7 molecule of non-coordinated methanol is refined per formula unit.

[Co₂(py2ald)₂](BF₄)₂·CH₃OH (2)

Pink hexagonal crystals of the complex were obtained by slow diethyl ether diffusion into a methanol solution of the ligand and cobalt(II) tetrafluoroborate. As the complex unit was found to be isomorphous to its perchlorate analogue, its projection is not depicted. Selected bond lengths and bond angles of compound **2** are presented in Table 3.1.

Table 3.1. Selected bond lengths and bond angles for [Co₂(py2ald)₂](ClO₄)₂·0.7CH₃OH (**1**) and [Co₂(py2ald)₂](BF₄)₂·CH₃OH (**2**)

<i>Bond lengths (Å)</i>	1	2		1	2
Co1 - N11	2.118(2)	2.112(3)	Co2 - N51	2.111(2)	2.099(3)
Co1 - N21	2.121(2)	2.124(3)	Co2 - N61	2.111(2)	2.105(3)
Co1 - N1	2.171(2)	2.174(3)	Co2 - N2	2.168(2)	2.168(3)
Co1 - O31	2.100(2)	2.100(3)	Co2 - O31	2.0343(18)	2.033(2)
Co1 - O71	2.0325(18)	2.033(2)	Co2 - O71	2.101(2)	2.094(2)
Co1 - O80	2.157(2)	2.161(3)	Co2 - O40	2.141(2)	2.146(2)

<i>Bond angles (°)</i>	1	2		1	2
O31 - Co1 - O71	78.32(7)	78.36(9)	O31 - Co2 - O40	87.97(8)	87.95(10)
O31 - Co1 - O80	162.24(7)	162.39(9)	O31 - Co2 - O71	78.25(8)	78.51(9)
O31 - Co1 - N1	91.61(9)	91.67(10)	O31 - Co2 - N2	166.29(8)	166.60(10)
O31 - Co1 - N11	103.97(8)	104.09(10)	O31 - Co2 - N51	111.58(8)	111.20(10)
O31 - Co1 - N21	95.94(9)	95.79(10)	O31 - Co2 - N61	94.43(8)	94.33(11)
O71 - Co1 - O80	87.41(8)	87.49(9)	O40 - Co2 - O71	162.73(7)	162.87(8)
O71 - Co1 - N1	165.10(8)	165.03(10)	O40 - Co2 - N2	102.95(8)	102.82(10)
O71 - Co1 - N11	93.04(8)	92.80(10)	O40 - Co2 - N51	82.18(9)	82.10(10)
O71 - Co1 - N21	113.45(8)	113.50(9)	O40 - Co2 - N61	86.69(9)	86.69(11)
O80 - Co1 - N1	104.30(9)	104.13(11)	O71 - Co2 - N2	92.30(8)	92.18(9)
O80 - Co1 - N11	87.14(9)	86.86(11)	O71 - Co2 - N51	93.16(8)	92.96(10)
O80 - Co1 - N21	79.97(10)	80.17(11)	O71 - Co2 - N61	104.54(8)	104.60(10)
N1 - Co1 - N11	78.62(9)	78.68(11)	N2 - Co2 - N51	78.52(9)	78.59(11)
N1 - Co1 - N21	78.20(8)	78.30(10)	N2 - Co2 - N61	78.20(9)	78.57(11)
N11 - Co1 - N21	149.70(9)	149.86(11)	N51 - Co2 - N61	151.16(9)	151.57(11)

[Mn₂(py2ald)₂](ClO₄)₂·C₄H₁₀O (3)

Bright-yellow rod-shaped crystals of the complex were obtained by slow diffusion of diethyl ether into a methanol solution of the ligand and manganese(II) perchlorate. An ORTEP projection of the complex is shown in Figure 3.3. The selected bond lengths and angles are presented in Table 3.2. The complex crystallizes in the

space group $P\bar{1}$ (no. 2). The unit cell includes one doubly charged complex cation, two perchlorate anions and one disordered molecule of diethyl ether. As in the case of the cobalt(II) complexes, two manganese ions are bridged by two oxygen atoms of deprotonated cresolate moieties, with a Mn1...Mn2 separation of 3.4013(10) Å. Each manganese(II) ion is further coordinated by two nitrogen donor atoms of two pyridine rings, the nitrogen atom of the tertiary amino group and the oxygen atom of the aldehyde group. The coordination spheres around both manganese ions can best be described as a trigonal prism, with torsion angles of 9.4°, 19.5° and 27.6° for the Mn1 ion, and 7.9°, 2.8° and 1.9° for the Mn2 ion. Two trigonal faces of the prism around the Mn1 ion are formed by the atoms N11, N1 and O31, and the atoms O80, O71 and N21. For the Mn2 ion, the two trigonal faces are formed by the atoms O31, O40 and N61, and the atoms N51, N2, O71. All Mn-N and Mn-O distances are in a normal range for high-spin ($S = 5/2$) manganese(II) complexes.⁴ In contrast to both cobalt complexes, non-coordinated counter ions do not exhibit any disorder.

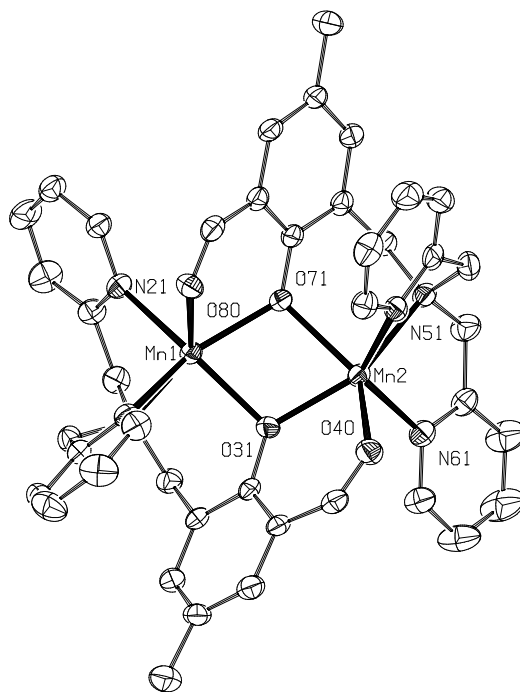


Figure 3.3. ORTEP projection of the complex cation $[\text{Mn}_2(\text{py}2\text{ald})_2]^{2+}$

$[\text{Cu}(\text{Hpy}2\text{ald})\text{Br}_2] \cdot 0.5\text{H}_2\text{O}$ (4)

A molecular plot of the complex is shown in Figure 3.4. Selected bond lengths and angles are presented in Table 3.3. As can be evidenced from the picture, the unit cell encloses two mononuclear formula units and one water molecule, which appears to be disordered over two positions with an occupancy factor of 0.50. These uncoordinated water molecules act as hydrogen bond donors with coordinated bromide anions as acceptors (see Table 3.5), thus resulting in the formation of centrosymmetric dimers with the formal composition $[\text{Cu}(\text{Hpy}2\text{ald})\text{Br}_2]_2 \cdot \text{H}_2\text{O}$.

Table 3.2. Selected bond lengths and bond angles for [Mn₂(py2ald)₂](ClO₄)₂·C₄H₁₀O (**3**)

<i>Bond lengths (Å)</i>			
Mn1 - N11	2.227(3)	Mn2 - N51	2.214(3)
Mn1 - N21	2.262(3)	Mn2 - N61	2.201(3)
Mn1 - N1	2.330(3)	Mn2 - N2	2.374(3)
Mn1 - O31	2.169(2)	Mn2 - O31	2.121(2)
Mn1 - O71	2.112(2)	Mn2 - O71	2.194(2)
Mn1 - O80	2.231(2)	Mn2 - O40	2.220(3)

<i>Bond angles (°)</i>			
O31 - Mn1 - O71	73.50(9)	O31 - Mn2 - O40	80.18(9)
O31 - Mn1 - O80	121.77(10)	O31 - Mn2 - O71	72.82(9)
O31 - Mn1 - N1	82.96(10)	O31 - Mn2 - N2	138.56(10)
O31 - Mn1 - N11	95.70(10)	O31 - Mn2 - N51	132.57(10)
O31 - Mn1 - N21	142.89(10)	O31 - Mn2 - N61	98.95(10)
O71 - Mn1 - O80	80.21(9)	O40 - Mn2 - O71	129.86(9)
O71 - Mn1 - N1	128.93(10)	O40 - Mn2 - N2	139.74(10)
O71 - Mn1 - N11	149.93(11)	O40 - Mn2 - N51	82.39(10)
O71 - Mn1 - N21	99.95(10)	O40 - Mn2 - N61	91.11(10)
O80 - Mn1 - N1	148.40(10)	O71 - Mn2 - N2	82.32(9)
O80 - Mn1 - N11	82.27(10)	O71 - Mn2 - N51	85.84(10)
O80 - Mn1 - N21	91.79(10)	O71 - Mn2 - N61	133.75(10)
N1 - Mn1 - N11	75.40(11)	N2 - Mn2 - N51	76.04(11)
N1 - Mn1 - N21	73.08(11)	N2 - Mn2 - N61	74.93(11)
N11 - Mn1 - N21	104.86(11)	N51 - Mn2 - N61	125.22(11)

The coordination environment around the copper(II) ion can be best described as either a very distorted octahedron with a Br₂N₃O donor set, or a square pyramid with a Br₂N₃ donor set and loosely bound phenol group. The phenol group of the cresol ring remains protonated, which disables it to form a bridge between two copper ions. This in turn results in the formation of the mononuclear complex. The oxygen atom O1 from the phenol group thus can be best regarded as only semi-coordinated to the Cu1 ion, with a very long Cu-O distance of 2.932(2) Å. It lies in one of the apical positions of an imaginary octahedron, with the second apical position being occupied by one of the bromide anions at a distance Cu1-Br1 of 2.7278(4) Å. The O1-Cu1-Br1 angle is 170.75(4)°. The equatorial plane is formed by the second bromide anion Br2, the nitrogen atom N1 from the tertiary amine group, and two nitrogen atoms N11 and N21 from the pyridine rings. The pyridine rings are located on either side of the ligand plane, thus being "trans" to each other. The interior angles N1-Cu1-N11 and N1-Cu1-N21 are

smaller than 90° ($81.03(8)^\circ$ and $81.05(8)^\circ$, respectively), due to the constraints imposed by the three-bond ligand-bite.

Besides the intermolecular hydrogen bonding, an intramolecular hydrogen bond is realized between the cresolic proton and the oxygen atom from the formyl group (the O1...O10 distance of 2.645 \AA , see also Table 3.5).

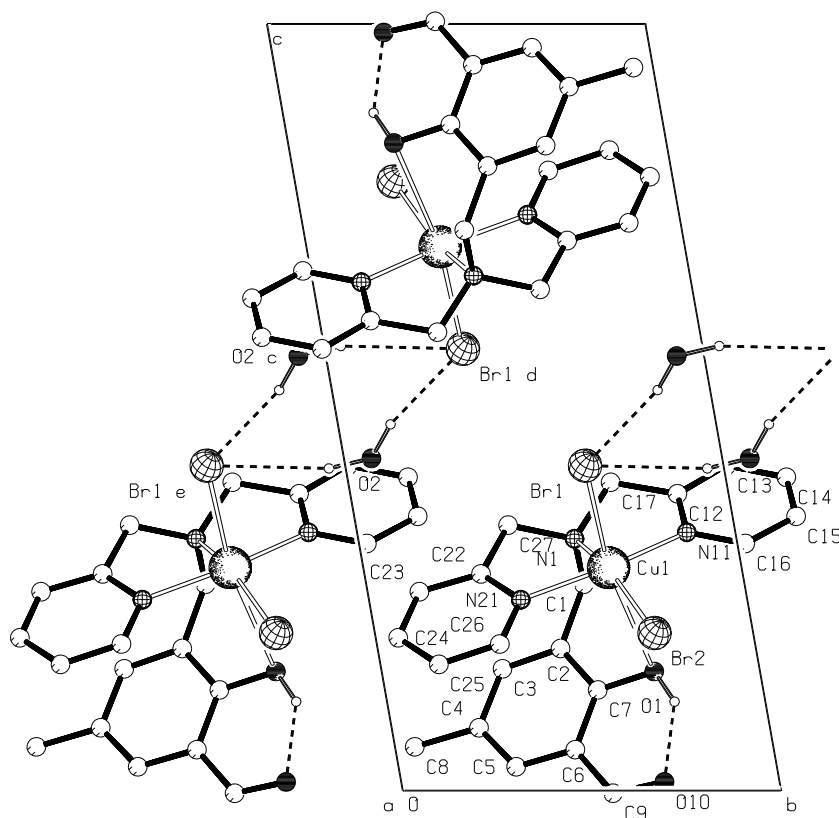


Figure 3.4. PLATON⁵ projection of the crystal structure of $[\text{Cu}(\text{Hpy2ald})\text{Br}_2] \cdot 0.5\text{H}_2\text{O}$ (**4**). The occupancy factor of each water molecule is 0.50. Only the hydrogen atoms participating in hydrogen bonding are shown.

$[\text{Mn}(\text{Hpy2ald})\text{Cl}_2]$ (5**)**

An ORTEP projection of the complex is shown in Figure 3.5. Selected bond lengths and angles are presented in Table 3.4. The structure of the complex looks very similar to that of complex **4**. However, in this case no intermolecular hydrogen bonding is present between the formula units. The coordination environment around the Mn1 ion can be described as a very distorted octahedron. The chloride anion Cl2 and the oxygen atom O31 from the cresol group are occupying the axial positions. Although the Mn1-O31 distance of $2.793(2) \text{ \AA}$ is shorter than the respective distance in complex **4** ($2.932(2) \text{ \AA}$), the oxygen atom can still be best regarded as only semi-coordinated to manganese ion.

Table 3.3. Selected bond lengths and bond angles for [Cu(Hpy2ald)Br₂] \cdot 0.5H₂O (**4**).

<i>Bond lengths (Å)</i>			
Cu1 - Br1	2.7278(4)	Cu1 - N1	2.0815(19)
Cu1 - Br2	2.4299(4)	Cu1 - N11	2.0170(19)
Cu1 - O1	2.932(2)	Cu1 - N21	2.0246(19)
<i>Bond angles (°)</i>			
Br1 - Cu1 - Br2	99.197(12)	Br2 - Cu1 - N21	97.42(6)
Br1 - Cu1 - O1	170.75(4)	O1 - Cu1 - N1	82.40(7)
Br1 - Cu1 - N1	100.65(5)	O1 - Cu1 - N11	78.43(7)
Br1 - Cu1 - N11	93.34(6)	O1 - Cu1 - N21	95.50(7)
Br1 - Cu1 - N21	93.63(5)	N1 - Cu1 - N11	81.03(8)
Br2 - Cu1 - O1	78.04(5)	N1 - Cu1 - N21	81.05(8)
Br2 - Cu1 - N1	160.15(5)	N11 - Cu1 - N21	161.69(8)
Br2 - Cu1 - N11	98.15(6)		

Similarly to the copper(II) bromide complex, the OH group of the cresolic moiety remains protonated. The Cl2-Mn1-O31 angle is 175.64(5)°. The basal plane of the octahedron is formed by two nitrogen atoms N11 and N21 from two pyridine rings, the nitrogen atom N1 from the tertiary amine group and the chloride anion Cl1 (the Mn-N distances vary in a range of 2.217(2)-2.360(2) Å, the Mn1-Cl1 distance is 2.3737(9) Å). Also in this compound an intramolecular hydrogen bond is realized between the hydrogen atom of the cresolic group and the oxygen atom from the formyl group, with an O31...O40 distance of 2.660 Å (see Table 3.5).

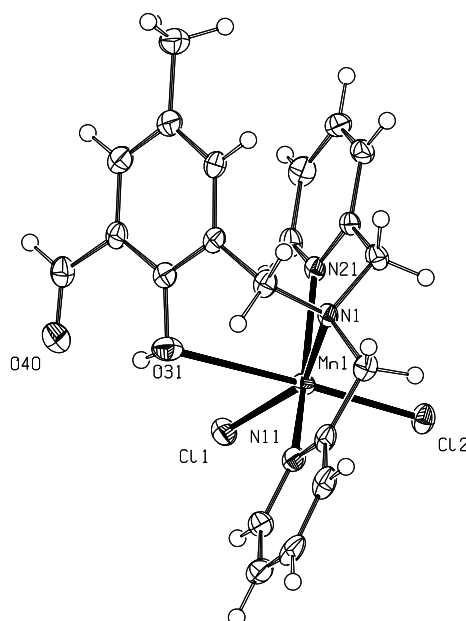
**Figure 3.5.** ORTEP projection of the crystal structure of [Mn(Hpy2ald)Cl₂] (**5**)

Table 3.4. Selected bond lengths and angles for [Mn(Hpy2ald)Cl₂] (**5**)

<i>Bond lengths (Å)</i>			
Mn1 - Cl1	2.3737(9)	Mn1 - N1	2.360(2)
Mn1 - Cl2	2.4078(8)	Mn1 - N11	2.217(2)
Mn1 - O31	2.793(2)	Mn1 - N21	2.223(2)
<i>Bond angles (°)</i>			
Cl1 - Mn1 - Cl2	106.07(3)	Cl2 - Mn1 - N21	94.92(6)
Cl1 - Mn1 - O31	76.21(5)	O31 - Mn1 - N1	75.92(7)
Cl1 - Mn1 - N1	151.89(5)	O31 - Mn1 - N11	78.07(7)
Cl1 - Mn1 - N11	104.33(6)	O31 - Mn1 - N21	88.15(7)
Cl1 - Mn1 - N21	102.28(6)	N1 - Mn1 - N11	73.27(8)
Cl2 - Mn1 - O31	175.64(5)	N1 - Mn1 - N21	73.22(7)
Cl2 - Mn1 - N1	101.98(5)	N11 - Mn1 - N21	145.95(8)
Cl2 - Mn1 - N11	97.70(6)		

Table 3.5. Hydrogen bonds D - H...A for [Cu(Hpy2ald)Br₂]₂·H₂O (**4**) and [Mn(Hpy2ald)Cl₂] (**5**)

	<i>Donor - H...Acceptor</i>	<i>D - H (Å)</i>	<i>H...A (Å)</i>	<i>D...A (Å)</i>	<i>D - H...A (°)</i>
	O1 - H10 .. O10	1.00(5)	1.82(5)	2.645(3)	137(4)
[Cu(Hpy2ald)Br ₂] ₂ ·0.5H ₂ O	O2 - H20 .. Br1 ⁱ	0.99	2.44	3.405(4)	164.2
	O2 - H30 .. Br1	0.95	2.70	3.592(4)	155.3
[Mn(Hpy2ald)Cl ₂]	O31 - H10 ... O40	0.72(3)	2.01(3)	2.660(3)	151(4)

i = 2-x, 1-y, 1-z

ii = x, 1-y, z

[Cu₂(py2ald)(μ-NO₃)(NO₃)₂]·CH₃CN (6**)**

An ORTEP projection of [Cu₂(py2ald)(μ-NO₃)(NO₃)₂]·CH₃CN is shown in Figure 3.6. Selected bond lengths and angles are given in Table 3.6. The dinuclear core is constituted by two copper ions (Cu...Cu distance 3.0652(6) Å) bridged on one side by an endogenous (μ-phenoxo) bridge and on the other side by an exogenous didentate nitrate anion. The complex shows both coordination number and donor-atom asymmetry. Cu1 is five coordinated with an almost ideal square pyramidal geometry (the parameter τ , which is used to describe the percentage of trigonal distortion from square pyramidal geometry, is 0.07 for the Cu1 ion; τ is 0 for an ideal square pyramid and 1 for an ideal trigonal bipyramid),⁶ and an N₃O₂ donor set. The basal plane is constituted by two *cis*-located oxygen atoms, O1 from the deprotonated cresolate and O32 from the bridging nitrate anion, and two *cis*-located nitrogen atoms, N1 of the

tertiary amine group and N20 of the pyridine ring. The nitrogen atom N10 from the other pyridine ring is occupying the apical position. The interior angles of the basal plane vary in a range of 82.07(9)-93.06(8)°. The distance Cu1...O41 is 3.031(3) Å and is perhaps too long to consider the O41 atom as a sixth ligand for the Cu1 ion.

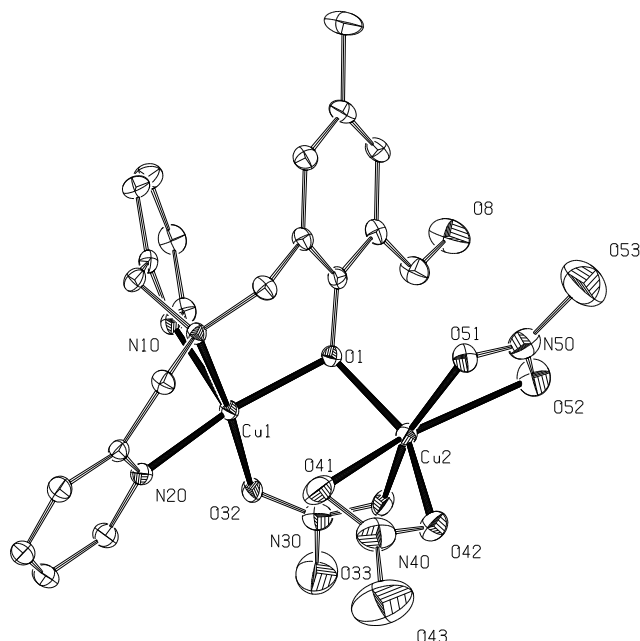


Figure 3.6. ORTEP projection of the crystal structure of $[\text{Cu}_2(\text{py2ald})(\mu\text{-NO}_3)(\text{NO}_3)_2]\cdot\text{CH}_3\text{CN}$ (**6**).

Hydrogen atoms and non-coordinated acetonitrile molecule are omitted for clarity.

The Cu2 ion is six coordinated with a very distorted octahedral geometry and an O_6 donor set. Only one of the oxygen atoms belongs to the ligand, whereas the five others are from three different nitrate anions. Two oxygen atoms O41 and O52 from two didentate chelating nitrate ions are occupying the axial positions, with long Cu-O bonds of 2.585(3) Å and 2.479(3) Å, respectively. The angle O41-Cu2-O52 is only 149.42(9)°, indicating a very large distortion from the regular octahedral geometry, apparently imposed by the small bite angle of the nitrate anions. The oxygen atoms O42 and O51 of two didentate chelating nitrate anions, the oxygen atom O1 of the deprotonated cresolate and the oxygen atom O31 of the didentate bridging nitrate anion lie in the equatorial plane, with Cu-O distances of 1.945(2)-1.978(2) Å. The interior angles of the equatorial plane are somewhat larger than 90°, viz. 90.26(10)-95.55(10)°. One non-coordinated molecule of acetonitrile is present in the crystal lattice.

3.2.2 Physical characterization

3.2.2.1 Mass-spectroscopy

Electrospray mass-spectra (ESI-MS) of both cobalt(II) complexes recorded in a methanol solution reveal one major peak at m/z 405, corresponding to $[\text{Co}_2(\text{py2ald})_2]^{2+}$ ($z = 2$). The experimentally observed isotopic pattern is in agreement with the

theoretically calculated one for $C_{42}H_{40}Co_2N_6O_4$. Similarly, in the ESI-MS spectrum of $[Mn_2(py2ald)_2](ClO_4)_2$ recorded in a methanol solution, a m/z 401 peak, corresponding to $[Mn_2(py2ad)_2]^{2+}$ ($z = 2$), can be found.

Table 3.6. Selected bond lengths and angles for $[Cu_2(py2ald)(\mu-NO_3)(NO_3)_2]CH_3CN$ (**6**)

<i>Bond lengths (Å)</i>			
Cu1 – O1	1.9918(19)	Cu2 – O2	1.959(2)
Cu1 - O32	1.937(2)	Cu2 - O31	1.945(2)
Cu1 – N1	2.041(2)	Cu2 – O41	2.585(3)
Cu1 - N10	2.199(2)	Cu2 - O42	1.946(2)
Cu1 - N20	1.999(2)	Cu2 - O51	1.978(2)
Cu1...O41	3.031(3)	Cu2 - O52	2.479(3)
<i>Bond angles (°)</i>			
O1 – Cu1 – O32	92.46(8)	O1 – Cu2 – O31	90.63(9)
O1 - Cu1 - N1	93.06(8)	O1 - Cu2 - O41	96.70(8)
O1 - Cu1 - N10	89.20(8)	O1 - Cu2 - O42	151.99(9)
O1 - Cu1 - N20	163.73(9)	O1 - Cu2 - O51	93.75(9)
O32 - Cu1 - N1	174.17(9)	O51 - Cu2 - O52	57.90(8)
O32 - Cu1 - N10	99.34(9)	O1 - Cu2 - O52	101.69(8)
O32 - Cu1 - N20	92.11(9)	O31 - Cu2 - O41	103.36(8)
N1 - Cu1 - N10	82.59(9)	O31 - Cu2 - O42	90.26(10)
N1 - Cu1 - N20	82.07(9)	O31 - Cu2 - O51	158.59(9)
N10 - Cu1 - N20	105.44(9)	O31 - Cu2 - O52	100.68(8)
Cu1 - O1 - Cu2	101.75(9)	O41 - Cu2 - O42	55.99(10)
		O41 - Cu2 - O51	96.94(8)
		O41 - Cu2 - O52	149.42(9)
		O42 - Cu2 - O51	95.55(10)
		O42 - Cu2 - O52	105.63(10)

The mass spectra of $[Cu(Hpy2ald)Br_2] \cdot H_2O$ and $[Mn(Hpy2ald)Cl_2]$, both recorded in methanol, are characterized by one major peak corresponding to the moiety $[M(Hpy2ald)X]^+$ (m/z 491 for $M = Cu$ and m/z 437 for $M = Mn$). These results are as expected and indicate that the solid-state structures of both complexes are retained in solution. It is also interesting to note that both Mn^{II} complexes are quite stable towards dioxygen in solution and can be easily isolated and recrystallized without undergoing the oxidation to Mn^{III} derivatives.

The mass spectra of $[Cu_2(py2ald)(\mu-NO_3)(NO_3)_2]$ were recorded for comparison in two different solvents (acetonitrile and methanol). The spectrum of the complex in acetonitrile solution shows two major peaks. The most intense one at m/z 596

corresponds to the fragment $[\text{Cu}_2(\text{py2ald})(\text{NO}_3)_2]^+$, in agreement with the solid-state structure of the complex. However, the second peak in the spectrum with only a slightly lower intensity (relative abundance 95%) at m/z 472, corresponds to the mononuclear fragment $[\text{Cu}(\text{Hpy2ald})\text{NO}_3]^+$. The discrimination between mononuclear and dinuclear fragments is unambiguous from the difference observed in the isotopic patterns, caused by the presence of one or two copper ions. The structure of the latter complex can be expected to look in general similar to the structure of the copper bromide complex, with the phenol group of the ligand being still protonated. The same two peaks are observed when the spectrum is recorded in methanol solution, thus it appears that the dinuclear complex with the deprotonated ligand exists in equilibrium with the mononuclear complex with the protonated ligand.

3.2.2.2 Ligand field spectroscopy

In the diffuse reflectance spectra of the powdered solids, for both cobalt complexes two major peaks are clearly visible. One of them, at approximately 420 nm, is a LMCT transition between the bridging phenoxo group and the metal ions and is typical for dinuclear complexes with phenol-based deprotonated ligands.^{7,8} The second peak, located at 1051 nm for the perchlorate complex and 1042 nm for the tetrafluoroborate complex corresponds to the ${}^4\text{T}_{2g} \leftarrow {}^4\text{T}_{1g}(\text{F})$ d-d transitions. In addition, in the spectra of both complexes another peak is observed at approximately 520 nm, as a shoulder of the LMCT transition band, which corresponds to the ${}^4\text{T}_{1g}(\text{P}) \leftarrow {}^4\text{T}_{1g}(\text{F})$ transition. The latter two bands are typical for d-d transitions in octahedrally surrounded Co^{II} ions.⁹ The positions of the bands are not significantly changing if the spectra are recorded in methanol, suggesting the absence of any significant modifications in the metal coordination sphere in solution. The diffuse reflectance spectrum of **3** is characterized by only one rather broad peak at 377 nm. It appears that the d-d transition band in octahedrally surrounded Mn^{II} is hidden by the LMCT band from the bridging phenoxo groups to the metal ions, which is usually observed around 400 nm.⁹ As in the case of both cobalt complexes, no significant changes were observed when the electronic spectrum was recorded in methanol.

In the diffuse reflectance spectrum of complex **4**, a fairly broad peak corresponding to a d-d transition of the Cu^{II} ions is observed at 750 nm with the shoulder around 940 nm. As shown previously, such spectroscopic behavior (high-energy absorption band in the visible region with a low-energy shoulder) is typical for square-pyramidal copper(II) complexes.¹⁰ Thus, the coordination sphere around the metal center can be indeed best described as square pyramidal. Another intensive band is observed at 378 nm. Taking into account that the OH group of the ligand is only semi-coordinated to the copper ion, and thus the LMCT band from the OH group to the metal ions is unlikely to be visible, this band has been assigned to the charge transfer from the bromide anions to the copper ions. Similarly, in the diffuse reflectance

spectrum of complex **5** a band is observed at 356 nm, which has been assigned to the charge transfer band from the chloride anions to the manganese ions. The d-d transition band in octahedrally surrounded Mn^{II} is known to be very weak, and must be hidden by the tail of the LMCT band, which is not uncommon.⁹ The diffuse reflectance spectrum of complex **6** is characterized by two major peaks. The first one, at 418 nm, corresponds to the LMCT transition of phenolate group to the copper ions.⁸ The second peak at 640 nm is in a normal range for d-d transitions of Cu^{II} ions.⁹

When the spectrum of complex **4** is taken in methanol solution, the position of the d-d band shifts somewhat towards the UV region (near 700 nm). Possible reasons for this shift can be additional solvation of the copper ions or the partial ligand exchange of the bromide anions with methanol molecules. The spectrum of $[\text{Mn}(\text{Hpy}2\text{ald})\text{Cl}_2]$ (**5**) remains unchanged if recorded in methanol.

For comparison, the spectrum of complex **6** was recorded in two different solvents: acetonitrile and methanol. When the spectrum is recorded in an acetonitrile solution, the position of the d-d transition band shifts to 672 nm ("red shift"). In methanol, this shift is even bigger (from 640 nm to 719 nm). These results suggest a change of the coordination sphere around the copper(II) ions in solution, presumably towards a square-pyramidal geometry.⁴ This observation appears to be in agreement with the results of mass-spectroscopic measurements, which also suggest the presence of significant amounts of mononuclear copper(II) species. As can be noticed, the position of the d-d band in the spectrum of complex **6** in a methanol solution is quite close to the position of the d-d band for complex **4**, which can be regarded as an additional evidence for the presence of mononuclear species similar in structure to complex **4**.

3.2.2.3 EPR spectroscopy on Cu^{II} complexes **4** and **6**.

The EPR spectrum of complex **4** in the solid state has a rhombic character, with $g_x = 2.05$, $g_y = 2.10$ and $g_z = 2.25$, suggesting a $d_{x^2-y^2}$ ground state. When the spectrum is recorded in a methanol glass, a hyperfine splitting becomes obvious. Three of four lines are easily observed (Figure 3.7, left, solid line), whereas the fourth is partially hidden in the $g_{x,y}$ region. The spectrum was simulated¹¹ (Figure 3.7, left, dashed line) using the parameters $g_x = 2.04$, $g_y = 2.06$, $g_z = 2.24$, $A_x \approx A_y \approx 0$ and $A_z = 18.4$ mT ($192 \times 10^{-4} \text{ cm}^{-1}$). These data suggest a distorted square-pyramidal surrounding for the Cu^{II} ions,¹² in agreement with the crystal structure of the complex.

One can also notice an additional peak at high field (approximately 330 mT), with a g -value below 2, in the spectrum of the complex. The appearance of this signal may indicate the presence of small amount of dinuclear copper(II) species in solution. Although the solid-state structure of the complex is essentially mononuclear, the partial formation of dinuclear species in solution due to the presence of potentially bridging bromide anions can be imagined. In this case, this absorption should originate from a

$\Delta M_s = \pm 1$ transition of the triplet spectrum.⁸ No signal corresponding to a $\Delta M_s = \pm 2$ transition could though be detected. As the structure of these presumably dinuclear species is unknown, the presence of this high-field signal was neglected during the simulation of the spectrum.

The EPR spectrum of compound **6**, recorded in the solid state at room temperature, exhibits one fairly broad isotropic signal with $g = 2.15$. No hyperfine splitting is resolved and no triplet signal is detected. The resolution does not improve upon cooling to liquid nitrogen temperature. A very similar spectrum is observed when the measurement is performed in a frozen acetonitrile solution. These data suggest an interaction between two copper(II) centers at relatively close positions, leading to exchange narrowing. However, when the spectrum is recorded in a methanol glass, it becomes much more complicated (Figure 3.7, right, solid line). The spectrum obviously indicates the presence of two different species in solution, and can be best regarded as an overlapping superposition of two rhombic spectra. In both cases, the $^{63,65}\text{Cu}$ hyperfine splitting in the g_z region can be observed, although some lines are partially hidden either due to the overlapping of two spectra with each other, or in the $g_{x,y}$ region. The resulting spectrum was satisfactorily simulated¹¹ (Figure 3.7, right, dashed line) considering two non-interacting Cu^{II} -containing species in an approximate ratio 1:1. For the species X, the simulating parameters are $g_x \approx g_y = 2.10$, $g_z = 2.44$, $A_x = 1.1$ mT ($10.1 \times 10^{-4} \text{ cm}^{-1}$), $A_y = 0$, $A_z = 10.9$ mT ($124.3 \times 10^{-4} \text{ cm}^{-1}$), and for the species Y, $g_x \approx g_y = 2.14$, $g_z = 2.26$, $A_x = 0$, $A_y = 0.43$ mT ($4.3 \times 10^{-4} \text{ cm}^{-1}$), and $A_z = 17.2$ mT ($181.5 \times 10^{-4} \text{ cm}^{-1}$).

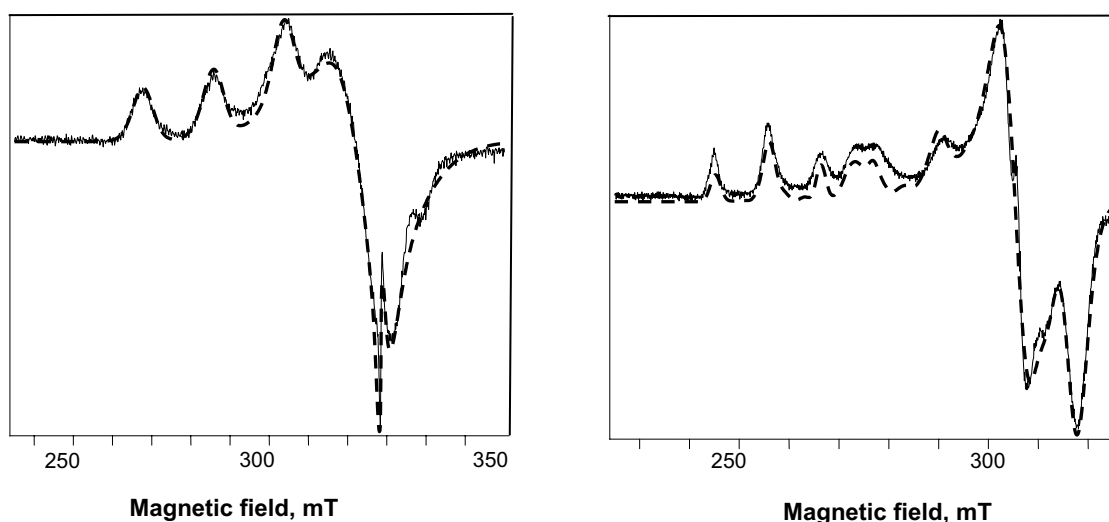


Figure 3.7. Left: X-band EPR spectrum of **4** (frozen methanol solution, 77 K, solid line) and the simulated curve¹¹ (dashed line). The sharp signal corresponds to the reference DPPH ($g = 2.0036$). Right: X-band EPR spectrum of **6** (frozen methanol solution, 77 K, solid line) and simulated curve¹¹ (dashed line).

Although the exact interpretation proved to be difficult, these parameters suggest a $d_{x^2-y^2}$ ground state for both species X and species Y. The simulation parameters for the species X are characteristic for elongated rhombic octahedral CuO_6 chromophores,⁴ and are very close to the values typical for Cu^{II} ions in methanol glass. The origin of this species can be Cu^{II} ions, coordinated by nitrate anions and/or, at least partially, by methanol molecules. The simulation parameters for the species Y are close to those for square-planar CuN_2O_2 chromophores. Thus, these results are in a good agreement with the presence in solution of a mononuclear species $[\text{Cu}(\text{Hpy}2\text{ald})\text{NO}_3]^+$, as suggested by mass and ligand field spectroscopy. However, it should be noticed that neither EPR, nor ligand field measurements provide any direct evidence confirming the presence of dinuclear species in solution as well. Thus, although the presence of dinuclear species was evidenced during the mass spectroscopic measurements, it can not be directly deduced from other spectroscopic techniques. Therefore another possibility, *i.e.* the complete dissociation of the dinuclear complex into mononuclear units of composition $[\text{Cu}(\text{Hpy}2\text{ald})\text{NO}_3]^+$ in methanol solution, can also not be excluded.

3.2.2.4 Magnetic susceptibility

Magnetic susceptibility measurements have been performed on crystals of **1** ($m = 16.99$ mg) and **2** ($m = 46.28$ mg) at 0.1 Tesla in the temperature range of 5 - 300 K. The plot of the χ^{-1} and χT versus the temperature (with χ being the magnetization per cobalt(II) ion) is shown in Figure 3.8. Because the magnetic behavior of the two compounds is almost identical, only the susceptibility curve of compound **1** is given.

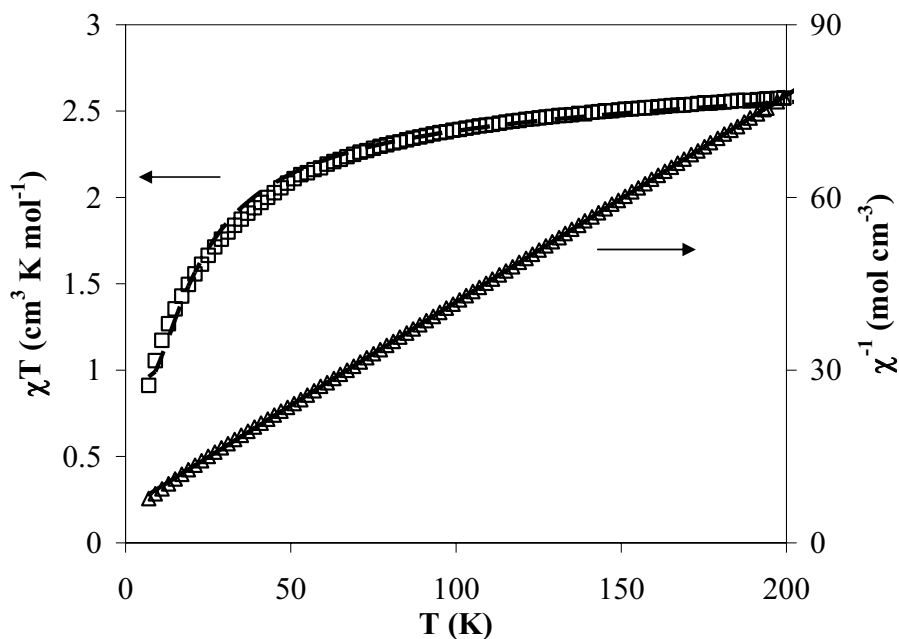


Figure 3.8. χT vs. T (\square) and χ^{-1} vs. T (Δ) curves of **1**. The solid line represents the linear fitting according the Curie-Weiss law, the dashed line represent the calculated lines for the parameters $g_1 = 2.31$, $-J_1 = 3.56$ cm^{-1} and $\theta_1 = 3.0$ K, with $R_1 < 7.9 \cdot 10^{-4}$.

At 300 K, $\chi_1 T = 2.59 \text{ cm}^3 \text{ K mol}^{-1}$, which is close to the expected value for a single, uncoupled cobalt(II) ion. The value of $\chi_1 T$ decreases upon cooling, going to zero at very low temperatures. The same behavior is observed for **2**, with a value for $\chi_1 T = 2.58 \text{ cm}^3 \text{ K mol}^{-1}$ at 300 K.

Fitting the linear part of the χ^{-1} vs. T curve (between 50 and 300 K) results in the Curie constants $C_1 = 2.63 \text{ cm}^3 \text{ K mol}^{-1}$ and $C_2 = 2.78 \text{ cm}^3 \text{ K mol}^{-1}$ and Curie-Weiss temperatures of $\theta_1 = -18.7 \text{ K}$ with $R_1 < 4.5 \cdot 10^{-6}$ and $\theta_2 = -16.5 \text{ K}$ with $R_2 < 8.7 \cdot 10^{-7}$ (the reliability factor R is defined as $R = n^{-1}[\Sigma(\chi_{\text{obs}} - \chi_{\text{cal}})^2 / (\chi_{\text{cal}})^2]$, where n = number of data points). The Curie constants correspond to g values of 2.36 for compound **1** and 2.43 for compound **2**.

The susceptibilities of **1** and **2** have been simulated over the entire temperature range using a modified Van Vleck equation (3.1)^{13,14} for a pair of coupled $S = 3/2$ spins (see Figure 3.8), where $x = \exp(-J/kT)$ and N , k and β have their normal values.¹⁵

$$\chi_M = \frac{g^2 N \beta^2}{k(T - \theta)} \times \frac{14 + 5x^6 + x^{10}}{7 + 5x^6 + 3x^{10} + x^{12}} + \text{TIP} \quad (3.1)$$

The observed and calculated susceptibilities are in agreement over the entire temperature range, applying the constants $g_1 = 2.31$, $-J_1 = 3.56 \text{ cm}^{-1}$ and $\theta_1 = 3.0 \text{ K}$, with $R_1 < 7.9 \cdot 10^{-4}$, for compound **1**, and the constants $g_2 = 2.32$, $-J_2 = 3.30 \text{ cm}^{-1}$ and $\theta_2 = 4.2 \text{ K}$, with $R_2 < 2.6 \cdot 10^{-4}$ for compound **2**.

The magnetic susceptibility of crystals of **3** (13.18 mg) has been measured between 5 and 250 K, with an external field of 0.1 Tesla. The plot of χ^{-1} and χT versus the temperature (with χ being the magnetization per manganese(II) ion) is shown in Figure 3.9. Also in this compound a decrease in magnetic susceptibility is observed with decreasing temperatures, from a value of $\chi T = 4.29 \text{ cm}^3 \text{ K mol}^{-1}$ at 250 K, to $1.4 \text{ cm}^3 \text{ K mol}^{-1}$ at 5 K. A Curie-Weiss behavior above 30 K results in a Curie constant $C_3 = 4.38 \text{ cm}^3 \text{ K mol}^{-1}$, which corresponds to a g value of $g_3 = 2.00$.

The magnetic susceptibility fit for the dinuclear manganese(II) system based on the isotropic Heisenberg model $H = 2J \cdot S_1 \cdot S_2$ ($S_1 = S_2 = 5/2$) is expressed by equation 3.2,¹⁶ where $x = \exp(-J/kT)$, and the other symbols have their usual meanings.¹⁵ The cryomagnetic properties of **3** are simulated well by equation 3.2, using the magnetic parameters $g_3 = 1.99$, $J_3 = 0.57 \text{ cm}^{-1}$ and $\text{TIP} = 0$. The reliability factor $R = 1.3 \cdot 10^{-5}$.

$$\chi_M = \frac{g^2 N \beta^2}{kT} \times \frac{x^{28} + 5x^{24} + 14x^{18} + 30x^{10} + 55}{x^{30} + 3x^{28} + 5x^{24} + 7x^{18} + 9x^{10} + 11} + \text{TIP} \quad (3.2)$$

Magnetic susceptibility measurements on powdered crystals of **4** ($m = 50.20 \text{ mg}$), **5** (19.04 mg) and **6** ($m = 29.11 \text{ mg}$) have also been performed at 0.1 Tesla. Values for χ in the copper(II) complexes have been calculated for dinuclear species.

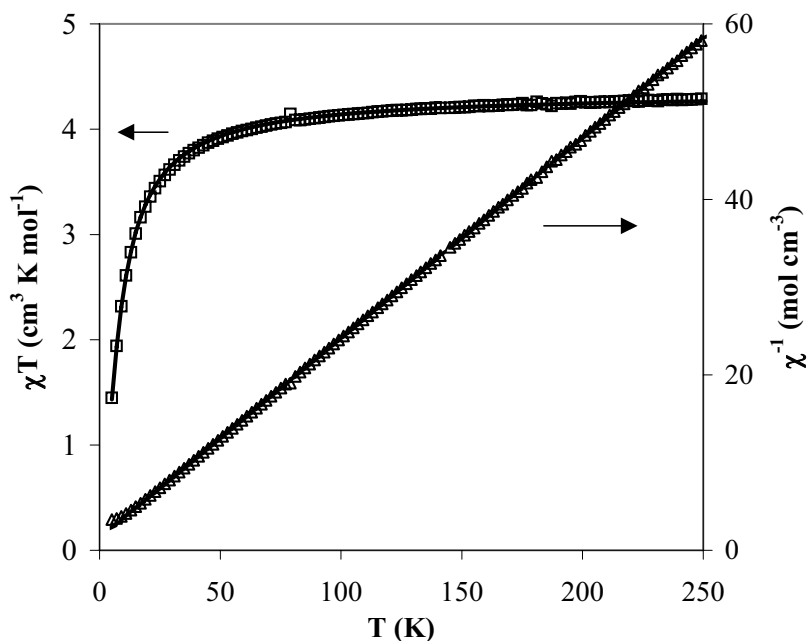


Figure 3.9. χT vs. T (\square) and χ^{-1} vs. T (Δ) curves of **3**. The solid line represents the linear fitting according the Curie-Weiss law, the dashed line represent the calculated lines for the parameters $g_3 = 1.99$, $J_3 = 0.57$ cm^{-1} , $\text{TIP} = 0$ and $R = 1.3 \times 10^{-5}$.

At 300 K, the χT for complex **4** is $0.84 \text{ cm}^3 \text{ K mol}^{-1}$. This value remains almost constant, as the compound shows a Curie-Weiss behavior over the entire temperature region. The Curie constant $C_2 = 0.42 \text{ cm}^3 \text{ K mol}^{-1}$ indicates a g -value of 2.12. The Curie temperature θ_2 is 0 K, as expected. Thus, no magnetic coupling is present between two mononuclear fragments coupled by the disordered water molecule.

For complex **5**, χT is $4.40 \text{ cm}^3 \text{ K mol}^{-1}$ at 300 K, corresponding to a magnetic moment of $5.93 \mu_B$. This value is in perfect agreement with the theoretically expected one for a high-spin Mn^{II} ion ($S = 5/2$). It remains unchanged over the entire temperature range, indicating a paramagnetic behavior of the complex, as could be predicted from its crystal structure. The Curie temperature θ is 0 K, as expected.

The plot of χ^{-1} and χT versus the temperature for complex **6** between 5 and 150 K (with χ being the magnetization per dinuclear complex) is shown in Figure 3.10. From the increase of the magnetic susceptibility at low temperature (from $\chi_6 T = 0.89 \text{ cm}^3 \text{ K mol}^{-1}$ at 150 K to $\chi_6 T = 1.05 \text{ cm}^3 \text{ K mol}^{-1}$ at 5 K) ferromagnetic behavior is evidenced. By linear regression, the Curie constant has been determined to be $C = 0.45 \text{ cm}^3 \text{ K mol}^{-1}$, which results in a g value of 2.18. This value is in a very good agreement with the one determined from EPR measurements in the solid state ($g = 2.15$).

A ferromagnetic interaction is usually observed, when the magnetic orbitals of two closely located metal ions have a negligible overlap, whereas the antiferromagnetic exchange is found when the magnetic orbitals are pointing towards each other in such a way that the overlap integral is reasonably large.^{17,18} In compound **6**, two unpaired

electrons from the Cu1 and Cu2 ions are both occupying $d_{x^2-y^2}$ orbitals. In a symmetrical complex, a bridging phenoxo group with an angle of $101.75(9)^\circ$ between the copper centers would normally result in an antiferromagnetic interaction. However, due to the asymmetry of the penta- and hexacoordinated copper(II) ions, induced by the ligand Hpy2ald and the nitrate anions, an overlapping of two $d_{x^2-y^2}$ orbitals can be expected to be very insignificant. In this case, a weak ferromagnetic exchange can be expected.

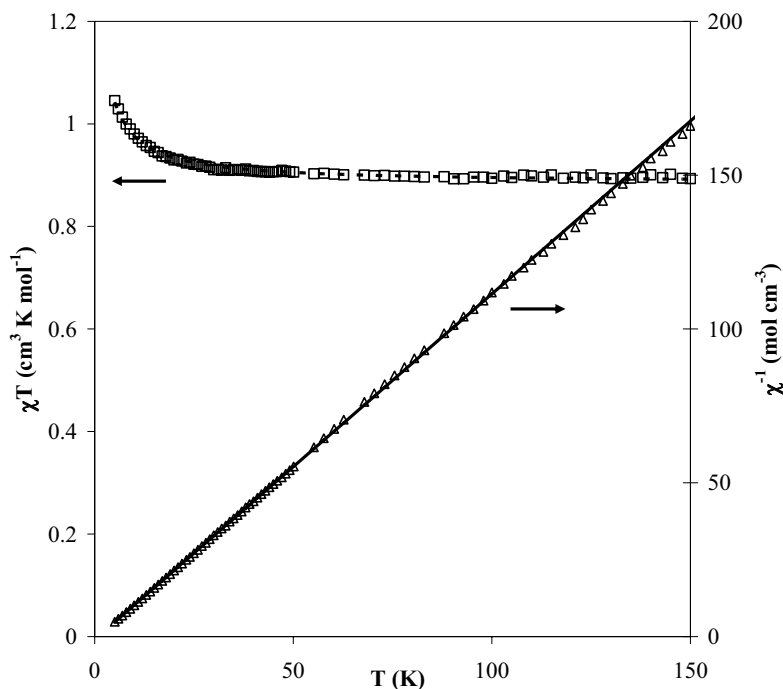


Figure 3.10. $\chi_1 T$ vs. T (\square) and χ_1^{-1} (Δ) vs. T curves of **6**. The solid line represents the linear fitting according to the Curie-Weiss law, the dashed line represent the calculated lines for the parameters $J_6 = 3.2 \text{ cm}^{-1}$, $g_6 = 2.17$ and $R = 1.24 \cdot 10^{-5}$.

The magnetic behavior has been simulated using the Bleaney-Bowers equation (3.3),^{15,19} in which $-J$ is the magnetic exchange parameter and all constants have their usual value.¹⁵

$$\chi_M = \frac{2g^2 N \beta^2}{kT [3 + \exp(-J/kT)]} + TIP \quad (3.3)$$

The best simulation is obtained with the values $J_6 = 3.2 \text{ cm}^{-1}$ and $g_6 = 2.17$. The reliability factor R is $1.24 \cdot 10^{-5}$.

3.3 Concluding remarks

The phenol-based ligand Hpy2ald contains a tridentate arm and a carbonyl group in two *ortho* positions with respect to the phenol group. Quite similar ligands and their Ni^{II} coordination compounds were previously described by Adams *et al.*¹ In the overwhelming majority of cases, the ligands reported by Adams were formed *in situ* by

the hydrolysis of an imino arm of the initially dinucleating phenol-based ligands.¹ The structures of the previously described complexes with this type of ligands include dinuclear metal cores, where two metals are doubly bridged by two phenolato groups. In all cases, the C=O group of the ligand is coordinated to the metal ion.¹

In the present chapter, six new cobalt(II), copper(II) and manganese(II) complexes with the ligand Hpy2ald are reported. Three of them (namely complexes **1**, **2** and **3**) possess structural features very similar to those reported by Adams *et al.*,¹ but the structures of the other three compounds are quite different. Thus, the reaction of Hpy2ald with copper(II) nitrate yields the asymmetric dinuclear complex [Cu₂(py2ald)(μ -NO₃)(NO₃)₂] \cdot CH₃CN (**6**), in which the two metal ions are doubly bridged by a deprotonated cresolate anion and a didentate nitrate anion. The metal to ligand ratio in this complex is 2:1, and the octahedral coordination environment of one of the copper ions is completed by chelating nitrate anions. The aldehyde group of the ligand remains non-coordinated.

The reaction of Hpy2ald with CuBr₂ yields the mononuclear complex of formal composition [Cu(Hpy2ald)Br₂] \cdot 0.5H₂O (**4**). In the crystal, the copper complexes form dimers by hydrogen bonding with lattice water molecules as hydrogen bond donors and coordinated bromides as acceptors. The metal-to-ligand ratio within a mononuclear fragment is 1:1. In this complex, the phenol group of the ligand remains protonated, failing to bridge two metal ions and instead being only semi-coordinated to one metal. As in the case of the nitrate complex, the aldehyde group is non-coordinated, but hydrogen bonded to the protonated phenol. The octahedral coordination environment around the metal ion is completed by nitrogen donor atoms of the tridentate arm from the ligand and two bromide anions.

Finally, the reaction of Hpy2ald with manganese(II) chloride yields the complex [Mn(Hpy2ald)Cl₂] (**5**). The molecular structure of this complex is very similar to the structure of the copper(II) bromide complex with intramolecular hydrogen bonding, but in this crystal lattice no intermolecular hydrogen bonding is present.

These unusual structural features of the latter three complexes open the possibility to speculate that the structure of complexes with carbonyl-containing phenol-based ligands is largely determined by the donor properties of the anion. Due to the presence of a very weak donor carbonyl group in the ligand, the counter ions present in the solution may compete with the oxygen atom of the carbonyl group for a place in the coordination sphere of the metal ion. Thus, the dinuclear core comprised of two metal ions and two ligands, in which the carbonyl group is coordinated to the metal ions, can only be formed if non-coordinating, or very weakly coordinating anions are present in the solution, as evident from the structures of the complexes **1**, **2** and **3**, containing perchlorate and tetrafluoroborate counter ions. At the same time, the presence of stronger donors, *e.g.* nitrate and halogen anions, prevents a weaker donor, *i.e.* the

carbonyl group, from coordinating to the metal ion. In addition, in all cases, changing the initial ratio of the reactants did not influence the structure of the formed complexes.

3.4 Experimental Section

3.4.1 Materials and Methods

All starting materials were commercially available and used as purchased. The synthesis of the ligand Hpy2ald is reported in Chapter 2. The infrared spectra of the complexes in the 4000-300 cm^{-1} range were recorded on a Bruker 330V IR spectrophotometer equipped with a Golden Gate Diamond. The ligand field spectra of the solids (300-2000 cm^{-1} , diffuse reflectance) and in solution were taken on a Perkin-Elmer 330 spectrophotometer equipped with a data station. Electrospray mass spectra (ESI-MS) in acetonitrile or methanol solution were recorded on a Thermo Finnigan AQA apparatus. X-band electron paramagnetic resonance (EPR) measurements were performed at room temperature and at 77 K in the solid state, or at 77 K as methanol frozen solutions on a Jeol RE2x electron spin resonance spectrometer, using DPPH ($g = 2.0036$) as a standard. Bulk magnetizations of polycrystalline samples were measured in the range 5-300 K with a Quantum Design MPMS-5S SQUID magnetometer, in a 1 kG applied field. The data were corrected for the experimentally determined contribution of the sample holder. Corrections for the diamagnetic responses of the complexes, as estimated from Pascal's constants, were applied.²⁰

3.4.2 Syntheses of the coordination compounds

[Co₂(py2ald)₂](ClO₄)₂·0.7CH₃OH (1): 20 ml of a methanol solution of cobalt(II) perchlorate (146 mg, 0.4 mmol) were added to 20 ml of a methanol solution of the ligand (69 mg, 0.2 mmol). Slow evaporation of the solvent yielded pink rectangular crystals suitable for X-ray crystal structure determination. Elemental analysis, % found (calc.) for [Co₂(py2ald)₂](ClO₄)₂·0.7CH₃OH (=C_{42.7}H_{42.8}Cl₂Co₂N₆O_{12.7}): C, 49.3 (49.7); H, 4.0 (4.2); N, 8.1 (8.0). IR, cm^{-1} : 3567 (O-H stretching); 2898 (C-H stretching); 1635 (C=O stretching); 1606, 1557 (C=N arom., C=C arom.), 1080 (ClO₄⁻)

[Co₂(py2ald)₂](BF₄)₂·CH₃OH (2): 20 ml of a methanol solution of cobalt(II) tetrafluoroborate (136 mg, 0.4 mmol) were added to 20 ml of a methanol solution of the ligand (69 mg, 0.2 mmol). Slow ether diffusion into the resulting pink solution yielded small pink hexagonal crystals of the complex which were found to be suitable for X-ray crystal structure determination. Elemental analysis, % found (calc.) for [Co₂(py2ald)₂](BF₄)₂·CH₃OH (=C₄₃H₄₃B₂Co₂F₈N₆O₃): C, 50.6 (50.8); H, 4.4 (4.4); N, 8.5 (8.3). IR, cm^{-1} : 2916 (C-H stretching); 1635 (C=O stretching); 1607, 1558 (C=N arom., C=C arom.); 1032 (BF₄⁻).

[Mn₂(py2ald)₂](ClO₄)₂·C₄H₁₀O (3): A solution of manganese(II) perchlorate (245 mg, 0.4 mmol) in 20 ml of methanol was added to a solution of the ligand (69 mg, 0.2 mmol) in 20 ml of methanol. Ether diffusion into the resulting bright-yellow solution led to the appearance of yellow rod-shaped crystals which were found suitable for X-ray crystal structure determination. Crystals were found to deteriorate rapidly when taken out of the mother solution, due to the loss of ether molecules from the crystal lattice. Elemental analysis, % found (calc.) for [Mn₂(py2ald)₂](ClO₄)₂ (= C₄₂H₄₀Cl₂Mn₂N₆O₁₂): C, 50.1 (50.4); H, 4.0 (4.0), N, 8.4 (8.4). IR, cm⁻¹: 2924 (C-H stretching); 1643 (C=O stretching); 1602, 1554 (C=N arom., C=H arom.), 1079 (ClO₄⁻).

[Cu(Hpy2ald)Br₂]·0.5H₂O (4): 20 ml of a methanol solution of the ligand (56 mg, 0.16 mmol) were added to an equal volume of a copper(II) bromide solution (72 mg, 0.32 mmol) in methanol. Green rectangular crystals appeared when the solvent was almost completely evaporated. Their quality was found to be suitable for X-ray diffraction analysis. Elemental analysis, % found (calc.) for [Cu(Hpy2ald)Br₂] (=C₂₁H₂₂Br₂CuN₃O_{2.5}): C, 43.9 (43.5); H, 3.8 (3.8); N, 7.5 (7.3). IR, cm⁻¹: ~3600, broad band (H₂O, asymmetric and symmetric OH stretching); 2980 (C-H stretching); 1654 (C=O stretching); 1608 (C=C arom., C=N arom.).

[Mn(Hpy2ald)Cl₂] (5): 20 ml of a methanol solution containing 129 mg (0.8 mmol) of manganese(II) chloride dihydrate were added to an equal volume of a methanol solution of the ligand (56 mg, 0.16 mmol). Slow evaporation of the resulting bright-yellow solution resulted in appearance of colorless crystals of the product. These crystals were found to be of sufficient quality for X-ray crystal structure determination. Elemental analysis, % found (calc.) for [Mn(Hpy2ald)Cl₂] (=C₂₁H₂₁Cl₂MnN₃O₂): C, 52.9 (53.3); H, 4.9 (4.5); N, 8.9 (8.9). IR, cm⁻¹: 2968 (C-H stretching); 1655 (C=O stretching); 1604 (C=C arom., C=N arom.).

[Cu₂(py2ald)(μ-NO₃)(NO₃)₂]·CH₃CN (6): 20 ml of an acetonitrile solution of the ligand (56mg, 0.16 mmol) were added to an equal volume of a copper(II) nitrate solution (77 mg, 32 mmol) in acetonitrile. Slow evaporation of the solvent led to the appearance of green rectangular crystals, which were of sufficient quality for X-ray structure determination. The crystals were found to deteriorate rapidly when taken out of the mother liquor, due to the loss of acetonitrile. Elemental analysis, % found (calc) for [Cu₂(py2ald)(μ-NO₃)(NO₃)₂] (=C₂₁H₂₀Cu₂N₆O₁₁): C, 37.9 (38.2); H, 3.4 (3.1); N, 12.8 (12.7). IR, cm⁻¹: 3047 (C-H stretching); 1610 (C=O stretching); 1550 (C=C arom., C=N arom.); 1436 (chelating didentate NO₃⁻, N=O stretching); 1283 (bridging didentate NO₃⁻, ν_a(NO₂)); 998 (bridging didentate NO₃⁻, ν_s(NO₂)).

3.4.3 X-ray crystallographic measurements

[Co₂(py2ald)₂](ClO₄)₂·0.7CH₃OH (1): (C₄₂H₄₀Co₂N₆O₄)(ClO₄)₂·0.7(CH₃O), Fw = 1031.99, red-brown block, 0.30×0.25×0.18 mm³, orthorhombic, *Fdd2* (no. 43), *a* = 27.0312(2) Å, *b* = 34.1008(2) Å, *c* = 18.9101(1) Å, *V* = 17431.05(19) Å³, *Z* = 16, ρ_{calc}.

= 1.573 g/cm³. 66127 reflections were measured on a Nonius KappaCCD diffractometer with rotating anode ($\lambda = 0.71073 \text{ \AA}$) at a temperature of 150(2) K up to a resolution of $(\sin\theta/\lambda)_{\max} = 0.61 \text{ \AA}^{-1}$; 8090 reflections were unique ($R_{\text{int}} = 0.040$). The structure was solved with Patterson methods (DIRDIF-97)²¹ and refined with SHELXL-97²² against F^2 of all reflections. Non-hydrogen atoms were refined freely with anisotropic displacement parameters. One perchlorate anion was refined with a disorder model. H atoms were refined as rigid groups; methanol H atoms were kept fixed. 634 refined parameters, 52 restraints. Flack x-parameter:²³ 0.005(9). $R [I > 2\sigma(I)]: R/ = 0.0285$, $wR2 = 0.0784$. $R [\text{all refl.}]: R/ = 0.0318$, $wR2 = 0.0806$. GoF = 1.040. Residual electron density between -0.36 and 0.46 e/\AA^3 . Molecular illustration, structure checking and calculations were performed with the PLATON package.⁵

[Co₂(py2ald)₂](BF₄)₂·CH₃OH (2): (C₄₂H₄₀Co₂N₆O₄)(BF₄)₂(CH₃O), Fw = 1016.32, brown block, 0.21×0.15×0.09 mm³, orthorhombic, *Fdd2* (no. 43), $a = 26.8533(2) \text{ \AA}$, $b = 33.8399(3) \text{ \AA}$, $c = 18.8585(1) \text{ \AA}$, $V = 17137.0(2) \text{ \AA}^3$, $Z = 16$, $\rho_{\text{calc.}} = 1.576 \text{ g/cm}^3$. 55275 reflections were measured on a Nonius KappaCCD diffractometer with rotating anode ($\lambda = 0.71073 \text{ \AA}$) at a temperature of 150(2) K up to a resolution of $(\sin\theta/\lambda)_{\max} = 0.59 \text{ \AA}^{-1}$; 7384 reflections were unique ($R_{\text{int}} = 0.053$). An absorption correction based on multiple measured reflections was applied ($\mu = 0.863 \text{ mm}^{-1}$, 0.85–0.92 transmission). Coordinates of compound **1** were taken as starting model and refined with SHELXL-97²² against F^2 of all reflections. Non-hydrogen atoms were refined freely with anisotropic displacement parameters. One BF₄ anion was refined with a disorder model. H atoms were refined as rigid groups. 608 refined parameters, 40 restraints. Flack x-parameter²³: -0.026(11). $R [I > 2\sigma(I)]: R/ = 0.0335$, $wR2 = 0.0790$. $R [\text{all refl.}]: R/ = 0.0411$, $wR2 = 0.0828$. GoF = 1.017. Residual electron density was between -0.44 and 0.71 e/\AA^3 . Molecular illustration, structure checking and calculations were performed with the PLATON package.⁵

[Mn₂(py2ald)₂](ClO₄)₂·C₄H₁₀O (3): (C₄₂H₄₀Mn₂N₆O₄)(ClO₄)₂(C₄H₁₀O), Fw = 1075.20, yellow block, 0.1×0.1×0.04 mm³, triclinic, $P\bar{1}$ (no. 2), $a = 12.6517(3) \text{ \AA}$, $b = 12.7867(3) \text{ \AA}$, $c = 16.7288(4) \text{ \AA}$, $\alpha = 85.068(2)^\circ$, $\beta = 75.6270(10)^\circ$, $\gamma = 65.4720(10)^\circ$, $V = 2384.55(10) \text{ \AA}^3$, $Z = 2$, $\rho_{\text{calc.}} = 1.497 \text{ g/cm}^3$. 14022 reflections were collected on a Bruker AXS Smart 6000 CCD diffraction system using Cu radiation ($\lambda = 1.54178 \text{ \AA}$) at a temperature of 153 K; 8009 reflections were unique ($R_{\text{int}} = 0.0390$). The structure was solved by direct methods using the program SHELXL-97.²² The final position of all non-hydrogen atoms were taken from a series of full-matrix least-squares refinement cycles based on F^2 with the SHELXL-97 program followed by difference Fourier synthesis.²² All non-hydrogen atoms, the counter ions and the ether solvent molecule were refined anisotropically. All hydrogen atoms were placed on calculated positions and allowed to ride on their corresponding atoms. The isotropic thermal parameters for the methyl protons were refined with 1.5 times and for all other hydrogen atoms with 1.2 times of the U_{eq} value of the bonding atom. 624 refined parameters, 0 restraints. $R [I$

$> 2\sigma(I)$]: $R I = 0.0516$, $wR2 = 0.1307$. R [all refl.]: $R I = 0.0706$, $wR2 = 0.1379$. GoF = 0.959. Residual electron density was between -0.67 and 0.91 e/Å³. Illustrations, structure calculations, and structure checking were performed with the PLATON package.⁵

[Cu(Hpy2ald)Br₂] \cdot 0.5H₂O (4): (C₂₁H₂₁Br₂CuN₃O₂)(H₂O)_{0.5}, Fw = 579.78, green block, 0.24 \times 0.18 \times 0.06 mm³, triclinic, $P\bar{1}$ (no. 2), $a = 7.7651(1)$ Å, $b = 8.8800(1)$ Å, $c = 16.9099(2)$ Å, $\alpha = 98.0365(6)^\circ$, $\beta = 93.0171(7)^\circ$, $\gamma = 112.7805(6)^\circ$, $V = 1057.19(2)$ Å³, $Z = 2$, $\rho_{\text{calc.}} = 1.821$ g/cm³. X-ray intensities were collected on a Nonius KappaCCD diffractometer with rotating anode ($\lambda = 0.71073$ Å, graphite monochromator) at a temperature of 150(2) K up to a resolution of $(\sin \theta/\lambda)_{\text{max}} = 0.65$ Å⁻¹. 14345 reflections were collected; 4758 reflections were unique. The structure was solved by automated Patterson methods (DIRDIF99)²⁴ and refined with SHELXL97²² against F^2 of all reflections. Non hydrogen atoms were refined freely with anisotropic displacement parameters. The phenolic hydrogen was located in the difference Fourier map and refined freely with isotropic displacement parameters. The water hydrogen atoms were located in the difference Fourier map and kept fixed in these positions. All other hydrogen atoms were refined as rigid groups by direct methods using the program SHELXL-97.²² R [$I > 2\sigma(I)$]: $R I = 0.0260$, $wR2 = 0.0595$. R [all refl.]: $R I = 0.0325$, $wR2 = 0.0625$. GoF = 1.036. Illustrations, structure calculations, and structure checking were performed with the PLATON package.⁵

[Mn(Hpy2ald)Cl₂] (5): (C₂₁H₂₁Cl₂MnN₃O₂), Fw = 473.25, yellow block, 0.56 \times 0.15 \times 0.03 mm³, triclinic, $P\bar{1}$ (no. 2), $a = 7.6829(14)$ Å, $b = 8.8364(11)$ Å, $c = 16.329(2)$ Å, $\alpha = 95.936(11)^\circ$, $\beta = 92.005(14)^\circ$, $\gamma = 111.789(13)^\circ$, $V = 1020.6(3)$ Å³, $Z = 2$, $\rho_{\text{calc.}} = 1.540$ g/cm³. 16182 reflections were collected on a Nonius KappaCCD diffractometer with rotating anode ($\lambda = 0.71073$ Å, graphite monochromator) at a temperature of 150(2) K up to a resolution of $(\sin \theta/\lambda)_{\text{max}} = 0.65$ Å⁻¹, of which 4640 reflections were unique. The structure was solved by automated Patterson methods (DIRDIF99)²⁴ and refined with SHELXL97²² against F^2 of all reflections. Non hydrogen atoms were refined freely with anisotropic displacement parameters. The phenolic hydrogen was located in the difference Fourier map and refined freely with isotropic displacement parameters. The water hydrogen atoms were located in the difference Fourier map and kept fixed in these positions. All other hydrogen atoms were refined as rigid groups by direct methods using the program SHELXL-97.²² R [$I > 2\sigma(I)$]: $R I = 0.0467$, $wR2 = 0.1098$. R [all refl.]: $R I = 0.0755$, $wR2 = 0.1225$. GoF = 1.037. Illustrations, structure calculations, and structure checking were performed with the PLATON package.⁵

[Cu₂(py2ald)(μ -NO₃)(NO₃)₂] \cdot CH₃CN (6): (C₂₁H₂₀Cu₂N₆O₁₁)(C₂H₃N), Fw = 700.56, dark green block, 0.48 \times 0.24 \times 0.18 mm³, monoclinic, $P2_1/c$ (no. 14), $a = 8.6632(7)$ Å, $b = 17.3510(10)$ Å, $c = 19.5299(17)$ Å, $\alpha = 90^\circ$, $\beta = 97.203(7)^\circ$, $\gamma = 90^\circ$, $V = 2912.5(4)$ Å³, $Z = 4$, $\rho_{\text{calc.}} = 1.598$ g/cm³. 51234 were collected on a Nonius

KappaCCD diffractometer with rotating anode ($\lambda = 0.71073 \text{ \AA}$, graphite monochromator) at a temperature of 150(2) K up to a resolution of $(\sin \theta/\lambda)_{\max} = 0.65 \text{ \AA}^{-1}$; 6695 reflections were unique. The structure was solved with direct methods (SHELXS97)²⁵ and refined with SHELXL97²² against F^2 of all reflections. Non hydrogen atoms were refined freely with anisotropic displacement parameters. Hydrogen atoms were refined as rigid groups by direct methods using the program SHELXL-97.²² $R [I > 2\sigma(I)]: R1 = 0.0408, wR2 = 0.1091. R [\text{all refl.}]: R1 = 0.0532, wR2 = 0.1172. GoF = 1.043.$ Illustrations, structure calculations, and structure checking were performed with the PLATON package.⁵

Crystallographic data for the structures of the complexes have been deposited with the Cambridge Crystallographic Data Centre as supplementary publication no. CCDC-216684 (compound **1**), 216685 (compound **2**), 216686 (compound **3**), 212531 (compound **4**), 212532 (compound **5**) and 212530 (compound **6**). Copies of the data can be obtained free of charge from the CCDC (12 Union Road, Cambridge CB2 1EZ, UK; tel: (+44) 1223-336-408; fax: (+44) 1223-336-003).

3.5 References

- (1) Adams, H.; Fenton, D. E.; Haque, S. R.; Health, S. L.; Ohba, M.; Okawa, H.; Spey, S. E. *J. Chem. Soc., Dalton Trans.* **2000**, 1849-1856.
- (2) Adams, H.; Clunas, S.; Fenton, D. E. *Inorg. Chem. Comm.* **2001**, 4, 667-670.
- (3) Koval, I. A.; Pursche, D.; Stassen, A. F.; Gamez, P.; Krebs, B.; Reedijk, J. *Eur. J. Inorg. Chem.* **2003**, 1669-1674.
- (4) *Comprehensive Coordination Chemistry*; Wilkinson, G., Ed.; Pergamon Press: Toronto, 1987; Vol. 5.
- (5) Spek, A. L. *J. Appl. Cryst.* **2003**, 36, 7-13.
- (6) Addison, A. W.; Rao, T. N.; Reedijk, J.; van Rijn, J.; Verschoor, G. C. *J. Chem. Soc., Dalton Trans.* **1984**, 1349-1356.
- (7) Gamez, P.; von Harras, J.; Roubeau, O.; Driessen, W. L.; Reedijk, J. *Inorg. Chim. Acta* **2001**, 324, 27-34.
- (8) Torelli, S.; Belle, C.; Gautier-Luneau, I.; Pierre, J. L.; Saint-Aman, E.; Latour, J. M.; Le Pape, L.; Luneau, D. *Inorg. Chem.* **2000**, 39, 3526-3536.
- (9) Lever, A. B. P. *Inorganic Electronic Spectroscopy*; 2 ed.; Elsevier: Amsterdam, 1984.
- (10) Rajendran, U.; Viswanathan, R.; Palaniandavas, M.; Laskiminaraya, N. *J. Chem. Soc., Dalton Trans.* **1994**, 1219-1226.
- (11) Neese, F.; *The program EPR, a modeling approach, Version 1.0*. University of Konstanz, 1993
- (12) Hathaway, B. J.; Billing, D. E. *Coord. Chem. Rev.* **1970**, 5, 143-207.
- (13) Emori, S.; Nakashima, H.; Mori, W. *Bull. Chem. Soc. Jpn.* **2000**, 73, 81-84.
- (14) Earnshaw, A. *Introduction to Magnetochemistry*; Acad. Press: London, 1968.
- (15) Kahn, O. *Molecular Magnetism*; Wiley-VCH: New York, 1993.
- (16) Sakiyama, H.; Sugawara, A.; Sakamoto, M.; Unoura, K.; Inoue, K.; Yamasaki, M. *Inorg. Chim. Acta* **2000**, 310, 163-168.
- (17) Hay, P. J.; Thibeault, J. C.; Hoffmann, R. *J. Am. Chem. Soc.* **1975**, 97, 4884-4899.
- (18) Kahn, O. *Angew. Chem. Int. Ed. Engl.* **1985**, 24, 834-850.
- (19) Bleaney, B.; Bowers, K. D. *Proc. R. Soc. London Ser. A* **1952**, 214, 451-465.
- (20) Kolthoff, I. M.; Elving, P. J. *Treatise on Analytical Chemistry*; Interscience Encyclopedia, Inc.: New York, 1963.
- (21) Beurskens, P. T.; Admiraal, G.; Beurskens, G.; Bosman, W. P.; Garcia-Granda, S.; Gould, R. O.; Smits, J. M. M.; Smykalla, C. *The DIRDIF97 program system, Technical Report of the Crystallography Laboratory, University of Nijmegen, The Netherlands.* **1997**.
- (22) Sheldrick, G. M.; *SHELXL-97, Program for the refinement of crystal structures*. University of Göttingen, Germany, 1997
- (23) Flack, H. D. *Acta Cryst.* **1983**, A39, 876.

- (24) Beurskens, P. T.; Admiraal, G.; Beurskens, G.; Bosman, W. P.; Garcia-Granda, S.; Gould, R. O.; Smits, J. M. M.; Smykalla, C. *The DIRDIF99 program system, Technical Report of the Crystallography Laboratory, University of Nijmegen, The Netherlands* **1999**.
- (25) Sheldrick, G. M.; *SHELXS-97, Program for crystal structure solution*. University of Göttingen, Germany, 1997

